Bacterial Leaf Blight (BLB) Disease Detection in the Municipality of Remedios T. Romualdez, Agusan Del Norte, Philippines using Multi-Spectral Data

Clarice Angela Boncales
Department of Geodetic Engineering, College of Engineering and Geosciences, Caraga State University

Aldwin Joshua Bondaog
Department of Geodetic Engineering, College of Engineering and Geosciences, Caraga State University

Arturo G. Cauba Jr.
Department of Geodetic Engineering, College of Engineering and Geosciences, Caraga State University

https://doi.org/10.5109/7395684

出版情報：Proceedings of International Exchange and Innovation Conference on Engineering & Sciences (IEICES). 11, pp.1340-1346, 2025-10-30. International Exchange and Innovation Conference on Engineering & Sciences
バージョン：

Bacterial Leaf Blight (BLB) Disease Detection in the Municipality of Remedios T. Romualdez, Agusan Del Norte, Philippines using Multi-Spectral Data

Clarice Angela Boncales[1], Aldwin Joshua Bondaog[1], Arturo G. Cauba Jr.[1, 2]
[1]Department of Geodetic Engineering, College of Engineering and Geosciences, Caraga State University, [2]Caraga Center for Geo-Informatics, Caraga State University
Email: agcauba@carsu.edu.ph

Abstract: *This study explored the use of multi-spectral satellite imagery and logistic regression to predict the spatial distribution of Bacterial Leaf Blight (BLB) in rice crops in Remedios T. Romualdez, Agusan del Norte, Philippines. Spectral index values were derived from PlanetScope imagery at ground-validated locations, highlighting variations in vegetation health. Logistic regression identified NPCI, PSRI, PSSRa, and GNDVI as significant predictors, with the final model achieving a strong Area Under the Curve (AUC) of 0.923. The generated spatial probability map of BLB aligned well with ground truth data from farmer interviews conducted during the June–November 2024 planting season, where reported infected fields matched high-probability areas on the map. This research demonstrates the potential of remote sensing and statistical modeling in accurately predicting BLB presence. The approach supports early detection and targeted disease management, helping reduce yield losses and improving decision-making for rice farmers in the region.*

Keywords: Remote Sensing, Multispectral imagery, Vegetation Indices, Bacterial Leaf Blight

1. INTRODUCTION

Rice (*Oryza sativa L.*) is the cornerstone in global food security serving as a primary dietary staple for over one-third of the world's population [1]. In the Philippines, rice cultivation is a vital component of the agricultural sector, contributing significantly to the national economy and the livelihoods of farmers [2],[3]. Throughout history, rice diseases have had a major effect on rice supply, often resulting in severe food shortages during serious epidemics [4]. Rice diseases have historically posed a significant threat to the global rice supply, leading to severe food shortages during epidemics [5]. The Philippines alone is one of the major producers of rice with a record 4.81 million hectares of area harvested for rice and total production of 19.96 million metric tons, according to the PSA 2021 [6]. For countries like the Philippines, it is heavily reliant on the production of rice to ensure local food supply and economic stability [7]. However, rice crops are susceptible to biotic and abiotic stresses that can greatly impact the yield and quality of rice. as per the report of International Rice Research Institute (IRRI), 37% of the rice yield loss is due to diseases [8]. The common diseases for rice in the Philippines are Rice Blast, Stem Rot, Sheath Rot, Bacterial Leaf Blight, and Tungro [9]. Among these diseases, Bacterial Leaf blight, caused by by a Gram-negative bacteria Xanthomonas oryzae pv. Oryza, is one of the most devastating pathogens of rice and is common in tropical and temperate regions especially in Asian countries [10], [11]. Traditional methods of identifying BLB relies heavily on visual inspections, which is prone to subjective judgement, time consuming, and only detect disease in the later stages when damage has already occurred. To address these limitation, there is a growing interest in utilizing remote sensing technology for crop health monitoring. The use of Multispectral Data, offer a non-destructive approach and potentially a more efficient way of monitoring crops health. Multispectral sensors capture data in multiple spectral bands, including those beyond the visible range, providing valuable information about the physiological status of plants that may be indicative of disease stress by utilizing vegetation indices to assess crop health [12], [13]. This study aims to explore the application of multispectral data for the identification of Bacterial Leaf Blight in rice crops in the municipality of RTR. By investigating the spectral signatures of healthy and BLB-infected rice plants, this research seeks to determine the effectiveness of multispectral data in accurately detecting and potentially mapping the disease in this important agricultural region. The objective of this study are to create a model for BLB rice disease detection, to generate a spatial distribution map showing the presence of Bacterial Leaf Blight in the rice fields of RTR and to evaluate the effectiveness of multispectral data in detecting Bacterial Leaf Blight in RTR's rice crops.

2. STUDY AREA

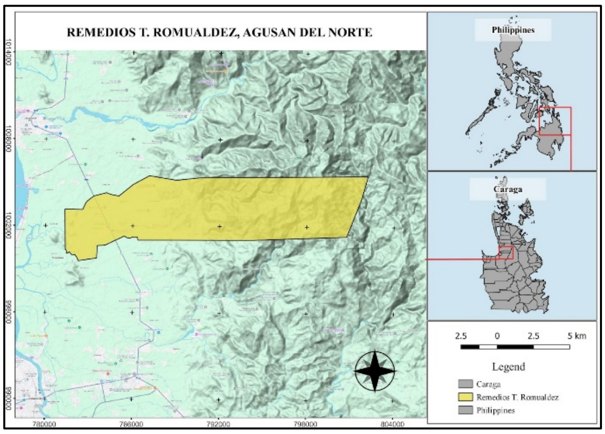

Figure 1. Map of the Study Area

Remedios T. Romualdez is a fifth-class municipality in the province of Agusan del Norte, Philippines. It has a population of 17,155 and a land area of 79.15 square kilometers, which constitutes to about 3.03% of the total land area of Agusan del Norte as per the 2020 census. It is situated around 9° 3' North latitude and 125° 35' East longitude. The elevation at this location is approximately 12.4 meters (or 40.7 feet) above the average sea level. Residents of RTR derive their income mainly from farming, as it is one of the leading rice producers of Agusan del Norte. More than 60% of the total area of RTR is dedicated to agricultural purposes and one of the leading crops produced by RTR is rice, with a total area of 1,750 hectares, followed by corn with an area of 1,100 hectares [14].

3. METHODS

3.1 Data Collection

Primary data regarding the presence of disease in the study area was obtained by interviewing the local farmers and field observation. The primary data consists of the field location of infected rice crops. Secondary data was acquired through PlanetScope. PlanetsScope was chosen due to its high spatial resolution of 3m x 3m, daily temporal resolution, and availability to students through their Education and Research Program, making it a suitable resource for agricultural monitoring.

The interview was conducted mainly due to the planting season (June to November 2024) had already commenced, limiting the opportunity for early-stage field data collection. Additionally, there was a lack of officially recorded incidences of Bacterial Leaf Blight (BLB) in the municipality. To address these limitations, farmers were interviewed to identify the locations of their rice fields and report any presence of BLB during the previous planting season. This approach provided essential ground truth information and supplemented the absence of formal records.

Table 1. Ground Truth Data

Respondent	Latitude	Longitude	Infected by BLB
Farmer_1	9° 3'6.49"N	125°35'59.30"E	Yes
Farmer_2	9° 3'31.95"N	125°34'1.58"E	Yes
Farmer_3	9° 3'24.94"N	125°36'11.60"E	Yes
Farmer_4	9° 2'52.22"N	125°34'7.44"E	Yes
Farmer_5	9° 4'28.87"N	125°36'53.59"E	Yes
Farmer_6	9° 3'44.15"N	125°36'58.95"E	Yes
Farmer_7	9° 3'42.62"N	125°36'1.11"E	Yes
Farmer_8	9° 4'36.31"N	125°36'3.19"E	Yes
Farmer_9	9° 4'18.45"N	125°36'13.79"E	Yes
Farmer_10	9° 3'3.76"N	125°36'2.42"E	Yes
Farmer_11	9° 3'7.32"N	125°36'9.30"E	Yes
Farmer_12	9° 3'18.60"N	125°36'3.51"E	Yes
Farmer_13	9° 3'36.49"N	125°36'10.90"E	Yes

3.2 Rice Mapping

The rice mapping process was conducted using the Google Earth Engine (GEE) Code Editor platform, which offers access to a wide range of satellite datasets and cloud-based geospatial processing capabilities. Sentinel-1 Synthetic Aperture Radar (SAR) imagery was utilized due to its ability to penetrate cloud cover and its dual polarization bands (VV and VH), which are particularly effective in distinguishing rice fields from other land cover types under various weather conditions.

To generate the rice map, Sentinel-1 images covering the June to November 2024 planting cycle season were selected and processed. Training ROI were manually digitized within the platform to represent known rice and non-rice areas based on field knowledge and visual interpretation. These ROIs were used to train a classification model, allowing the algorithm to identify spectral and backscatter patterns unique to rice paddies.

Once the model was trained, it was applied across the study area to classify and map rice fields. The resulting rice map provided a spatial overview of rice cultivation within the study period, forming a foundational layer for further analysis, including disease detection.

3.3 Rice Mapping

Multispectral data often contains errors such as distortions and noise in the satellite image. It is crucial to address these issues to ensure suitability for further analysis and model training, ultimately leading to better performance and more reliable results. PlanetScope, which is a commercial satellite imagery service operated by Planet Labs, offers high-resolution, daily global coverage with frequent revisit capabilities. Its preprocessed imagery is orthorectified and radiometrically corrected, ensuring consistency across localized atmospheric conditions and minimizing spectral uncertainty over time and location making it analysis ready [15]. Despite these preprocessing steps, the images may still contain clouds that can hinder accurate analysis of rice crops. To address this, the acquired PlanetScope imagery was uploaded to the Google Earth Engine Code Editor platform, where image clipping and cloud masking were performed. Cloud removal was facilitated using the Usable Data Masks (UDM2) provided by Planet, which help identify and mask out clouds, shadows, haze, and snow—thereby improving the usability and reliability of the imagery for crop monitoring [16].

3.4 Feature Extraction and Analysis

After cloud masking, the calculation of vegetation indices was conducted using the same GEE Code Editor Platform. The Vegetation indices and their corresponding formulae used are as follows:

Table 2. Vegetation Indices and their Formulae

Vegetation index	Formula	Sources
Normalized Difference Vegetation Index (NDVI)	((NIR-Red)/(NIR+Red))	[15]
Green Normalized Difference Vegetation Index (GNDVI)	((NIR-Green)/(NIR+Green))	[16]
Normalized Green-Red Difference Index (NGRDI)	((Green-Red)/(Green+Red))	[17]
Plant Senescence Reflectance Index (PSRI)	((Red-Green)/NIR)	[18]

Normalized Pigment Chlorophyll Index (NPCI)	((R_680-R_430)/(R_680+R_430))	[19]
Normalized Difference Red Edge (NDRE)	((NIR-RedEdge)/(NIR+Red Edge))	[20]
Pigment Specific Simple Ratio (chlorophyll a) (PSSRa)	(NIR/Red)	[21]

3.5 Logistic Regression Analysis and Model Evaluation

After the calculation of index value of each infected and healthy points, logistic regression analysis was carried out using JASP Statistical Analysis Software. Prior to the analysis, a new variable was created to serve as the binary dependent variable, where healthy samples were coded as '0' and those infected with Bacterial Leaf Blight (BLB) were coded as '1'. This binary classification allowed the logistic regression model to predict the likelihood of BLB presence based on the spectral index values derived from the satellite imagery.

The main objective of employing logistic regression was to develop a model that could identify significant predictors—specifically vegetation indices—that are strongly associated with the presence of BLB in the area. By identifying which variables contribute most to the probability of infection, the model aids in pinpointing early indicators of disease and helps in targeted field management. Depicted below is formula in calculating the probability:

$$P(Y=1\mid X) = \frac{1}{1+e^{-(\beta_0+\beta_1 X_1+\beta_2 X_2+\ldots\beta_n X_n}}$$

Equation 1. Binary Logistic Regression Formula

Where π indicates the probability an event occurring, while βi denotes the regression coefficients linked to the reference group and the explanatory variables Xi

After the model was developed, trained, and tested, the QGIS software platform was used to calculate the probability of BLB infection using the logistic regression model. To assess the accuracy and reliability of the resulting distribution map, the farmers' point locations obtained from the interviews were overlaid onto the map. The results were carefully examined to determine whether the points correctly aligned with the predicted infection areas.

4. RESULTS AND DISCUSSIONS

4.1 Rice Mapping and Spectral Index Calculation

The rice mapping process successfully generated a spatial distribution map of rice fields in RTR, Agusan del Norte, for the June to November 2024 planting season. Using Sentinel-1 SAR imagery accessed through the Google Earth Engine (GEE) Code Editor platform, the classification was able to distinguish rice paddies from other land cover types with high clarity despite frequent cloud cover during the rainy season.

The resulting rice map (Figure 3), showed a high concentration of rice fields in easternmost part of the municipality. In contrast, the western portion is dominated by mountainous terrain, indicating that rice cultivation is primarily concentrated in the lowland areas. This spatial pattern demonstrates a clear separation between agricultural zones and non-agricultural or upland regions. Areas consistently showing high VV and VH backscatter signatures during key crop growth periods were identified as active rice paddies.

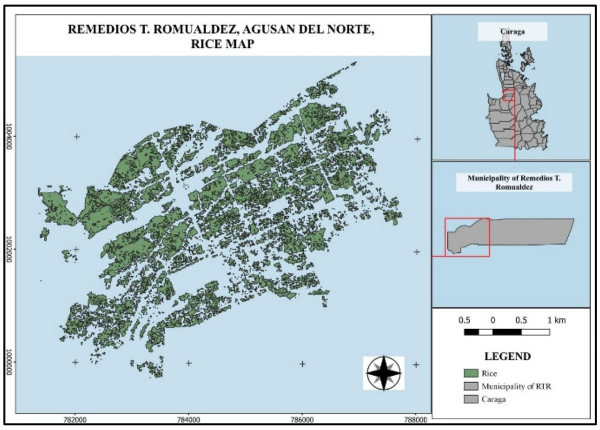

Figure 2. RTR Rice Map 2024

Using the formulas outlined in Table 3, the spectral index values for each of the ground truth points (Table 2) were calculated using multispectral imagery within the Google Earth Engine Code Editor platform. Notably, indices such as NDVI, and GNDVI which are indicators of vegetation greenness and biomass, exhibit a range of values across the sampled locations. Similarly, indices related to vegetation stress and pigment content, such as NGRDI, PSRI, and NPCI, also show variability. The NDRE and PSSRa indices, often sensitive to chlorophyll content and canopy structure, also display a spectrum of values. These variations suggest potential differences in vegetation health and condition across the sampled rice paddies within the study area.

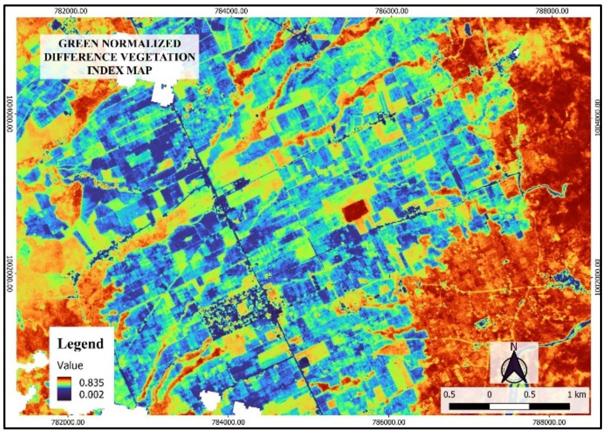

Figure 3. Green Normalized Difference Vegetation Index (GNDVI)

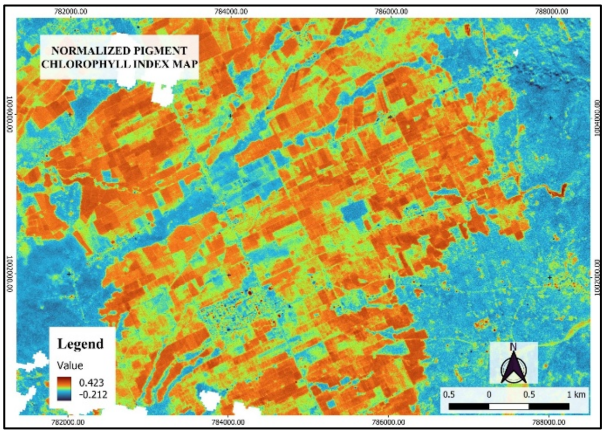

Figure 4. Normalized pigment chlorophyll ration index (NPCI)

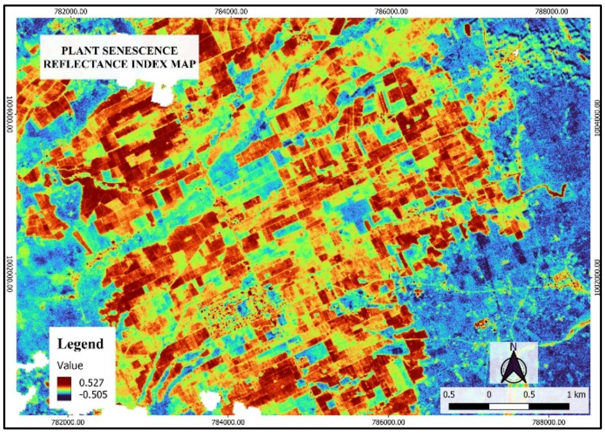

Figure 5. Plant senescence reflectance index (PSRI)

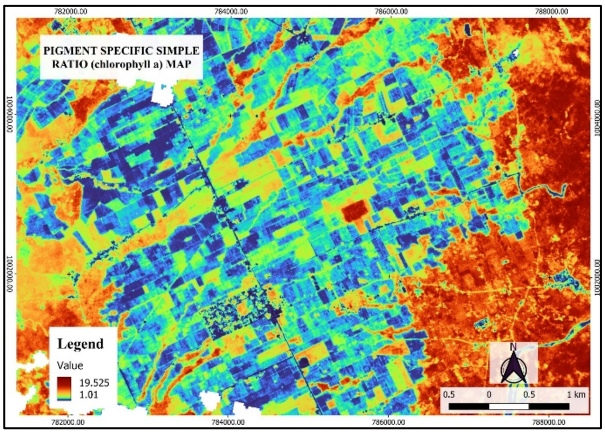

Figure 6. Pigment Specific Simple Ratio (chlorophyll index) (PSSRa)

4.2 Logistic Regression and Model Evaluation

To model the relationship between the spectral indices and the presence of BLB rice disease, a series of logistic regression models were developed and evaluated. The figure below presents the summary statistics for these models and displays the coefficients of the final selected model (M_2).

Logistic Regression

Model Summary - class

Model	Deviance	AIC	BIC	df	ΔX^2	p	McFadden R^2	Nagelkerke R^2	Tjur R^2	Cox & Snell R^2
M_0	69.737	71.737	73.669	50			0.000		0.000	
M_1	55.602	59.602	63.465	49	14.135	< .001	0.203	0.325	0.244	0.242
M_2	52.830	58.830	64.625	48	2.772	0.096	0.242	0.379	0.300	0.282
M_3	43.578	51.578	59.305	47	9.252	0.002	0.375	0.538	0.414	0.401
M_4	35.465	45.465	55.124	46	8.113	0.004	0.491	0.657	0.551	0.489

Coefficients

					Wald Test		
Model	Parameter	Estimate	Standard Error	z	Wald Statistic	df	p
M_0	(Intercept)	0.276	0.283	0.977	0.955	1	0.329
M_1	(Intercept)	−1.364	0.632	−2.158	4.655	1	0.031
	NPCI	24.498	8.250	2.966	8.796	1	0.003
M_2	(Intercept)	1.275	1.686	0.756	0.572	1	0.450
	NPCI	17.948	8.817	2.036	4.144	1	0.042
	PSRI	10.749	6.548	1.641	2.694	1	0.101
M_3	(Intercept)	4.597	2.345	1.961	3.844	1	0.050
	NPCI	21.856	11.013	1.985	3.939	1	0.047
	PSRI	40.003	14.157	2.826	7.984	1	0.005
	PSSRa	0.454	0.178	2.547	6.486	1	0.011
M_4	(Intercept)	5.468	2.855	1.915	3.668	1	0.055
	NPCI	38.336	15.444	2.484	6.168	1	0.013
	PSRI	37.895	16.528	2.293	5.257	1	0.022
	PSSRa	1.167	0.409	2.852	8.136	1	0.004
	GNDVI	−13.971	5.840	−2.392	5.723	1	0.017

Note. class level "1" coded as class 1.

Performance Diagnostics

Performance metrics

	Value
AUC	0.923

Figure 7. Logistic Regression Analysis Result Generated from JASP software

The progression of logistic regression models (M_0 to M_4) demonstrates the increasing predictive power as spectral indices are added. The significant decrease in deviance and AIC, along with the increase in pseudo-R^2 values (McFadden, Nagelkerke, Tjur, and Cox & Snell), indicates improved model fit with the inclusion of more predictors. The significant chi-square (ΔX^2) values for M_1, M_3, and M_4 ($p < 0.05$) confirm that these models provide a statistically significant improvement over the null model (M_0).

Based on the model selection criteria, Model M_4, which includes NPCI, PSRI, PSSRa, and GNDVI (Green Normalized Difference Vegetation Index), appears to be the most robust for predicting BLB occurrence. It exhibits the highest pseudo-R^2 values, indicating the best overall fit to the data among the tested models. All four spectral indices are statistically significant predictors of BLB presence ($p < 0.05$). The positive coefficients for NPCI, PSRI, and PSSRa suggest that higher values of these indices increase the likelihood of BLB, while the negative coefficient for GNDVI indicates that lower greenness is associated with a higher probability of infection, which aligns with expectations for diseased vegetation. The high AUC of 0.923 indicates excellent model performance in distinguishing between healthy and BLB-infected rice.

$$P(Y = 1 \mid X) = \frac{1}{5.468 + 38.356NPCI + 37.895PSRI + 1.167PSSRa - 13.971GNDVI}$$

Equation 2. Model-derived Formula

4.3 BLB Spatial Distribution Map

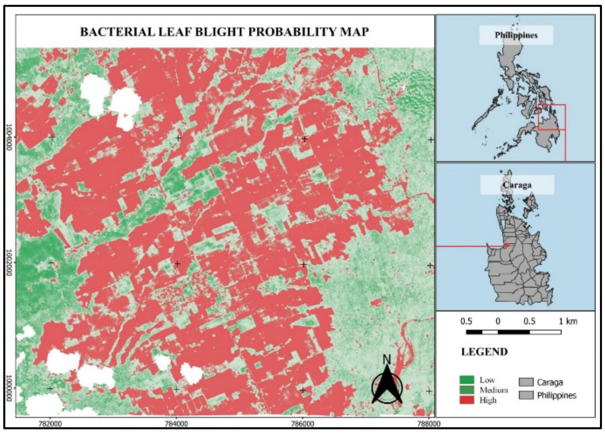

Figure 8. BLB Distribution Map of RTR, Agusan del Norte

As depicted in Figure 8, the BLB Spatial Distribution Map visually represents the predicted likelihood of Bacterial Leaf Blight occurrence across the rice-growing landscape of RTR, Agusan del Norte. The color gradient, transitioning from cooler blue and green hues to warmer yellow and red tones, illustrates a spectrum of increasing BLB risk as predicted by the logistic regression model. Areas depicted in red and dark red signify the highest predicted probability of BLB infection, suggesting that the combination of spectral characteristics in these locations strongly indicates the potential presence of the disease. Conversely, the blue and green areas represent zones where the model predicts a lower likelihood of BLB (Healthy). The spatial arrangement of these risk zones reveals a non-uniform distribution, with clusters of high-risk areas interspersed with regions of lower risk, potentially reflecting underlying spatial variations in environmental conditions or agricultural practices within the area. This map serves as a crucial tool for targeted disease management efforts, enabling prioritized scouting and early intervention in high-risk zones.

4.4 Validation

The overlaid ground truth data on the BLB Spatial Distribution Map was used to provide a crucial visual assessment of the model's predictive accuracy. The ground truth data used was the data acquired from the farmers through interview if there was an incidence during the June-Nov 2024 planting season.

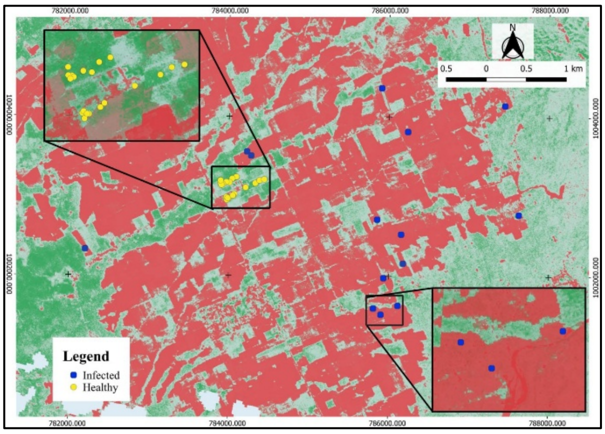

Figure 9. Validation of BLB Distribution Map in RTR by Overlaying Points from Farmers

Table 3. Confusion Matrix

		Predicted	
Actual		0	1
	0	5	5
	1	0	13

Based on the validation results presented in Figure 9 and the confusion matrix, the logistic regression model's predictive capability for Bacterial Leaf Blight (BLB) infection was effectively evaluated. The spatial distribution map was overlaid with ground truth points obtained through field interviews, where infected and healthy rice paddies were denoted as 1 and 0, respectively. The infected points (white circles) predominantly fell within the red to orange zones—areas with higher predicted probabilities of infection. In contrast, healthy points (magenta circles) were mainly located in cooler zones (green to blue hues), indicating lower risk. To quantitatively evaluate the model's predictive accuracy, a confusion matrix was generated to assess whether the model correctly classified the validation points. The model successfully identified all 13 infected samples, resulting in a sensitivity (true positive rate) of 100%. Additionally, it correctly classified 5 out of the 10 healthy points, achieving a specificity (true negative rate) of 50%. While the model still exhibits a slight tendency to over predict infection—misclassifying 5 healthy samples as infected—its ability to consistently detect actual infected areas highlights its potential as a valuable early warning tool for Bacterial Leaf Blight (BLB) presence.

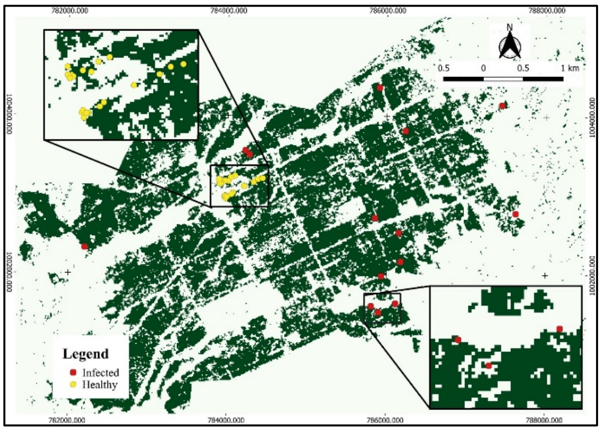

Figure 10. Validation of Points Overlain on the Rice Map

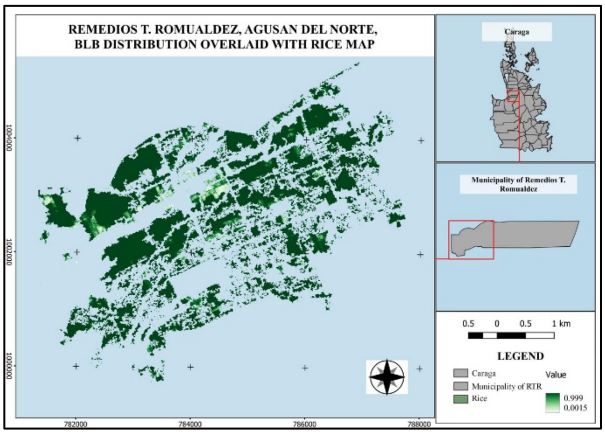

Figure 11. RTR BLB Distribution Map Overlaid with Rice Map

Depicted in Figure 12, the distribution map is overlaid with the rice map to visualize the predicted spread of Bacterial Leaf Blight (BLB) within actual rice cultivation areas. The majority of the rice fields exhibit dark green hues—ranging from medium sea green to dark green—indicating a high probability of BLB infection across much of the area. In contrast, zones represented by light green, which signify a lower probability of infection or healthy conditions, appear only in limited portions of the map. This spatial pattern suggests a widespread potential for disease presence, emphasizing the need for targeted monitoring and management within the affected zones.

5. CONCLUSION

This study successfully demonstrated the potential of combining high-resolution satellite imagery and spectral indices with logistic regression modeling to detect and map Bacterial Leaf Blight (BLB) infection in rice crops within RTR, Agusan del Norte. Spectral indices derived from PlanetScope imagery, particularly NPCI, PSRI, PSSRa, and GNDVI, were found to be statistically significant predictors of BLB presence.

The generated BLB spatial distribution map revealed spatial patterns of potential infection, with high-risk zones prominently visualized using a red-to-blue color gradient. Validation through overlaid farmer-identified ground truth points further confirmed the model's reliability—infected locations closely corresponded with high-probability areas on the map, affirming the model's robustness in identifying real-world disease occurrences. Overall, the integration of remote sensing, statistical modeling, and ground truth data offers a practical and scalable method for early detection and monitoring of BLB in rice farming systems.

6. REFERENCES

[1] L. C. S. Asube, C. A. Bentozal, G. J. C. Malaluan, and J. E. Gesta, "The Peri-Urban Sprawl: Characterization and Analysis of Rice Cropland Conversion Using Remote Sensing and GIS Techniques in Butuan City," *Int. Exch. Innov. Conf. Eng. Sci.*, vol. 10, pp. 171–176, 2024, doi: 10.5109/7323259.

[2] J. M. Tecson and J. O. Lucnod, "Energy Inputs and Economic Analysis of Organic and Inorganic Rice Production in Agusan Del Sur, Philippines," *Int. Exch. Innov. Conf. Eng. Sci.*, vol. 10, pp. 105–111, 2024, doi: 10.5109/7323250.

[3] L. Kong, J. Liang, X. Hu, M. Li, and S. Bai, "Variation and Enlightenment of Sown Area of Rice Varieties in Rice Research Institute of Guangdong Academy of Agricultural Sciences," *Guangdong Agricultural Sciences*, vol. 49, no. 9, 2022, doi: 10.16768/j.issn.1004-874X.2022.09.018.

[4] F. Wang, "Achievements and Prospects of Hybrid Rice Breeding —Review of 50 Years'Research on Hybrid Rice by Rice Research Institute of Guangdong Academy of Agricultural Sciences," 2020. doi: 10.16768/j.issn.1004-874X.2020.12.001.

[5] S. Conde, S. Catarino, S. Ferreira, M. P. Temudo, and F. Monteiro, "Rice Pests and Diseases Around the World: Literature-Based Assessment with Emphasis on Africa and Asia," Apr. 01, 2025, *Multidisciplinary Digital Publishing Institute (MDPI)*. doi: 10.3390/agriculture15070667.

[6] M. F. Stuecker, M. Tigchelaar, and M. B. Kantar, "Climate variability impacts on rice production in the Philippines," *PLoS One*, vol. 13, no. 8, 2018, doi: 10.1371/journal.pone.0201426.

[7] N. M. Neyra-Cabatac, J. M. Pulhin, and D. B. Cabanilla, "Indigenous agroforestry in a changing context: The case of the Erumanen ne Menuvu in Southern Philippines," *For Policy Econ*, vol. 22, 2012, doi: 10.1016/j.forpol.2012.01.007.

[8] M. M. Kalai Priya and S. Dhanabal, "Analyses of Nine Different Types of Diseases in Paddy with Hybrid Algorithms using Deep Learning." [Online]. Available: www.ijert.org

[9] R. M. Pascual, M. Roque, S. G. Canonigo, J. Nobleza, and L. R. Cruz, "Development of mobile application for automatic identification of biotic diseases in Oryza sativa using image processing techniques," in *Proceedings - 2020 International Symposium on Computer, Consumer and Control, IS3C 2020*, 2020. doi: 10.1109/IS3C50286.2020.00131.

[10] D. R. A. Sanya *et al.*, "A review of approaches to control bacterial leaf blight in rice," 2022. doi: 10.1007/s11274-022-03298-1.

[11] S. A. H. Naqvi, U. ud D. Umar, A. Hasnain, A. ur Rehman, and R. Perveen, "Effect of Botanical Extracts: A Potential Biocontrol Agent for Xanthomonas Oryzae Pv. Oryzae, Causing Bacterial Leaf Blight Disease of Rice," *Pakistan Journal of Agricultural Research*, vol. 32, no. 1, 2019, doi: 10.17582/journal.pjar/2019/32.1.59.72.

[12] J. P. Dash, G. D. Pearse, and M. S. Watt, "UAV multispectral imagery can complement satellite data for monitoring forest health," *Remote Sens (Basel)*, vol. 10, no. 8, 2018, doi: 10.3390/rs10081216.

[13] M. Pla *et al.*, "Calibrating sentinel-2 imagery with multispectral UAV derived information to quantify damages in mediterranean rice crops caused by western swamphen (Porphyrio porphyrio)," *Drones*, vol. 3, no. 2, 2019, doi: 10.3390/drones3020045.

[14] "Income Classification: 5 th Class Employment Labor Force Population: 8,780 Employment Rate: 62% Major Fields of Employment % of Employed Population."

[15] R. W. H. Rouse, J. A. W. Haas, and D. W. Deering, "'aper A 20 MONITORING VEGETATION SYSTEMS IN THE GREAT PLAINS WITH ERTS."

[16] S. M. Moges, W. R. Raun, R. W. Mullen, K. W. Freeman, G. V. Johnson, and J. B. Solie, "Evaluation of green, red, and near infrared bands for predicting winter wheat biomass, nitrogen uptake, and final grain yield," *J Plant Nutr*, vol. 27, no. 8, 2004, doi: 10.1081/PLN-200025858.

[17] C. J. Tucker, "Red and photographic infrared linear combinations for monitoring vegetation," *Remote Sens Environ*, vol. 8, no. 2, 1979, doi: 10.1016/0034-4257(79)90013-0.

[18] Y. J. Lee, C. M. Yang, K. W. Chang, and Y. Shen, “A simple spectral index using reflectance of 735 nm to assess nitrogen status of rice canopy,” *Agron J*, vol. 100, no. 1, 2008, doi: 10.2134/agronj2007.0018.

[19] M. N. Merzlyak, A. A. Gitelson, O. B. Chivkunova, and V. Y. Rakitin, “Non-destructive optical detection of leaf senescence and fruit ripening,” *Physiol Plant*, vol. 106, no. 1, 1999.

[20] E. M. Barnes *et al.*, “Coincident detection of crop water stress, nitrogen status and canopy density using ground based multispectral data,” in *Proc. 5th Int. Conf. Precis Agric*, 2000.

[21] G. A. Blackburn, “Spectral indices for estimating photosynthetic pigment concentrations: A test using senescent tree leaves,” *Int J Remote Sens*, vol. 19, no. 4, 1998, doi: 10.1080/014311698215919.